In-Situ Estimation of MOCVD Growth Rate via a Modified Kalman Filter

Wilbur W. Woo and Spyros A. Svoronos
Dept. of Chemical Engineering, University of Florida, Gainesville, FL 32611

Haluk O. Sankur and Jagmohan Bajaj
Rockwell International Corporation, Science Center, Thousand Oaks, CA 91360

Stuart J. C. Irvine
Multi Disciplinary Research and Innovation Centre, North East Wales Institute Plas Coch, Wrexham, Clwyd LL 11 2AW, U.K.

In-situ laser reflectance monitoring of metal-organic chemical vapor deposition (MOCVD) is an effective way to monitor growth rate and expitaxial layer thickness of a variety of III-V and II-VI semiconductors. Materials with low optical extinction coefficients, such as ZnTe/GaAs and AlAs/GaAs for a 6328 Å HeNe laser, are ideal for such an application. An extended Kalman filter modified to include a variable forgetting factor was applied to the MOCVD systems. The filter was able to accurately estimate thickness and growth rate while filtering out process noise and cope with sudden changes in growth rate, reflectance drift, and bias. Due to the forgetting factor, the Kalman filter was successful, even when based on very simple process models.

Introduction

The II-VI semiconductor ZnTe is used as a buffer layer between a GaAs substrate and a CdTe epitaxial layer to reduce defect concentration and ensure (100) growth on a (100) substrate. The thickness of the buffer layer is very important to the operability of the final device and is a major cause of manufacturing defects. AlAs is often used with GaAs to make compound semiconductor devices, and the thickness of this layer is also very important to the operability of the final device. Implementation of an *in-situ* monitoring device in either of these cases would help keep the thickness within desired specifications and help monitor crystal quality, cutting manufacturing waste and cost. The operating pressures involved in metal-organic chemical vapor deposition (MOCVD) that exceed 0.9 torr, however, make the electron- and ion-beam-based *in-situ* monitoring techniques commonly used in molecular-beam epitaxy unusable.

Light, however, is unaffected by the operating pressures of MOCVD. Two light-based methods finding increasing usage are ellipsometry and reflectometry. Ellipsometry involves the reflection of elliptically polarized light from the surface of the sample, causing a change in polarization. A brief review of ellipsometry is given by Rhiger (1993). Specular laser reflectance, where the intensity of a laser beam reflected off a growing epitaxial film is measured, has been used to successfully monitor growth of a variety of II-VI and III-V systems. Three studies used a 6,328-Å HeNe laser (Jensen et al., 1988; Irvine et al., 1989, 1994), while a fourth used a frequency-doubled argon ion laser (Sankur et al., 1991). Other studies that have used optical techniques similar to the one here for the estimation of film thicknesses are those by Alius and Schmidt (1990), Boebel and Möller (1993), Breiland et al. (1995), and Morrison (1995). In other work, similar techniques have been used in etching processes (Wong and Boning, 1995; Boning et al., 1994; Deaton and George, 1987; Sternheim et al., 1983). The on-line measurement used in the present work is reflectance from a 6,328-Å HeNe laser at near-normal incidence angle.

An extended Kalman filter (EKF) estimates the state variables—film thickness and growth rate—of a nonlinear dynamic mathematical model of a process by minimizing the mismatch between the estimated and measured outputs, for example, reflectance intensity. The performance of a conven-

Correspondence concerning this article should be addressed to S. A. Svoronos.

tional EKF is highly dependent on the ability of the model to predict any changes in the state variables, especially sudden ones, whether they are due to outside disturbances or changes in manipulated variables. A method to help overcome this problem has been used in the paper industry and involves a recursive least-squares algorithm interacting with an EKF (Wang et al., 1993). Here the conventional EKF is modified by incorporating a variable forgetting factor, which allows the filter to overcome the inadequacies of the model and produce estimates comparable to those from an EKF using a more complex model. The modified EKF is applied to the MOCVD process to estimate film thickness and growth rate.

Experimental Methods

In MOCVD, a carrier gas, usually hydrogen, transports metalorganic or hydride precursors into the reactor. Metalorganics are introduced into the carrier gas by passing it through a bubbler containing that liquid or solid precursor. Hydrides, such as arsine and phosphine, commonly used as group V precursors, are gaseous and are introduced directly into the carrier gas. In a vertical reactor, the precursors approach the substrate perpendicularly to the surface, while in a horizontal reactor, the flow is parallel. On the surface of the heated substrate, a pyrolytic reaction takes place, depositing the semiconductor material.

The ZnTe/GaAs system was grown in an atmospheric pressure horizontal reactor with rotation capability. It included an optical window flushed with dry helium gas. Diethyl zinc was the group II precursor, and diisopropyl telluride was used as the group VI precursor. A 2-mW, high-stability, HeNe laser operating at 6,328 Å was directed at near-normal incidence angle on the wafer. A 15-Hz beam chopper was placed between the laser and the wafer. The reflected light intensity was recorded with a low-noise silicon detector and a lock-in amplifier.

The AlAs/GaAs data were obtained using a vertical MOCVD reactor at atmospheric pressure and 750°C. It was equipped with a 6,328-Å HeNe laser and similar intensity measuring equipment as the previously mentioned system. The precursors were trimethyl aluminum (TMA) and arsine.

State and Output Models

Output model

The ideal reflectance from a normal incidence beam R_{ideal} is a function of the wavelength of the incident laser light, the deposited film thickness, the refractive index of the incident medium, and the complex refractive index of the film, $N_f = n_f - ik_f$, where n_f and k_f are the refractive index and extinction coefficient of the film, respectively (Macleod, 1986; Bajaj et al., 1993). If the laser wavelength is constant and if the film is of constant composition, reflectance intensity becomes a function only of film thickness. When this is applied to a growing film, an oscillating reflectance intensity results where the refractive index determines the amplitude and frequency, and the extinction coefficient determines the damping rate. It should be stressed that the ideal reflectance is dependent on the composition profile of the film stack. In this study, however, only the deposition of a single layer with uniform properties is considered, greatly simplifying the calculations.

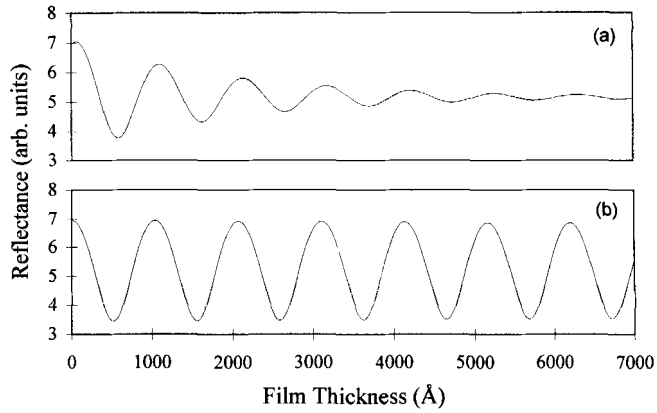

Figure 1. Ideal reflectance vs. time for (a) a growing CdTe film and (b) a growing ZnTe film.

The extinction coefficient is important because observability, or the ability to estimate the states (thickness and growth rate) from the measurements is lost whenever the reflectance becomes constant with respect to time, including the local extrema of the oscillations. The value of k is dependent on the interband photon absorption. The bandgap energy at room temperature of ZnTe is 2.26 eV, and that of AlAs is 2.16 eV, both of which are greater than the photon energy of 1.96 eV of the 6,328-Å laser used. This results in a very small extinction coefficient for both materials ($k_{ZnTe} < 0.01$, $k_{AlAs} \approx 0.003$) allowing sustained oscillations over large film thickness. Figure 1 shows the effect of the extinction coefficient where (a) is the ideal reflectance intensity from a growing CdTe film on GaAs ($n_{CdTe} = 3.04$, $k_{CdTe} = 0.253$) and (b) is the ideal reflectance from a growing ZnTe film ($n_{ZnTe} = 3.06$, $k_{ZnTe} < 0.01$).

The ideal reflectance is easily calculated, but does not allow for deviations that can be caused by crystal defects or other process noises. The addition of bias and drift terms make the model more flexible and the filter more robust. The relative drift term was modeled as first order with respect to time, and the bias was considered an additive term making the final output reflectance intensity R_{out}

$$R_{out} = R_{ideal}(1 - \beta t) - \alpha, \tag{1}$$

where β is the drift coefficient, α the bias coefficient, and t the elasped time since the EKF was started, typically the beginning of growth.

Simple state model

The EKF for both systems was initially based on a simple four-state model. The first two states model the growth of the epitaxial layer and are growth rate g and thickness θ. Thickness propagates as

$$\frac{d\theta}{dt} = g, \tag{2}$$

while the growth rate was modeled as constant giving

$$\frac{dg}{dt} = 0. \tag{3}$$

A better model would predict changes in growth rate.

The third and fourth state variables are the drift and bias in the output signal. Since variations in α and β are not modeled, their nominal dynamics are

$$\frac{d\alpha}{dt} = \frac{d\beta}{dt} = 0, \tag{4}$$

making the EKF the only mechanism changing these states.

Improved state model

As stated earlier, a better model would predict changes in growth rate, improving the performance of the EKF. A process model with five state variables was implemented on the AlAs/GaAs system. In this model, film growth was considered strictly mass-transfer-limited so that growth rate was proportional to the trimethyl aluminum (TMA) concentration in the growth chamber C_{Al}, that is,

$$\frac{d\theta}{dt} = \gamma C_{Al}, \tag{5}$$

where γ is a growth coefficient. The growth coefficient was modeled as being constant and the TMA concentration was modeled as having a first-order plus time-delay response to bubbler flow rate giving

$$\frac{d\gamma}{dt} = 0 \tag{6}$$

$$\frac{dC_{Al}}{dt} = -\frac{1}{\tau}C_{Al} + \frac{K_b}{\tau}u(t-D), \tag{7}$$

where τ is a time constant, u the TMA bubbler flow rate, K_b the bubbler steady-state gain, and D the delay. These parameters were not estimated by the EKF, but were assigned values on the basis of known carrier flow rates and semiempirical calculations. The fourth and fifth states were the reflectance intensity drift and bias parameters used in the simple model.

Modifications to the Extended Kalman Filter

When testing the conventional continuous-discrete EKF (Gelb, 1974) on ZnTe/GaAs with the simple model, it was found that the filter could not cope with the inadequacies of the model. The EKF was tested with an experimental run during which the growth rate was purposely changed several times by varying either the group II bubbler flow rate, or the group VI bubbler flow rates or the bubbler temperatures. The filter was not able to adjust to large, sudden changes in the growth rate. A mechanism was needed to increase the filter's ability to deal with changes in the process. This problem has been addressed in the least-squares estimator by the use of variable forgetting factors.

Recursive least-squares estimation (RLS) is the conventional method for estimating constant or slowly changing parameters. To allow the estimator to track possible changes in the parameter values, RLS is often used with a variable forgetting factor. The equivalence of the RLS and the EKF (Goodwin and Sin, 1984; Åström and Wittenmark, 1988) motivates us to adapt the Fortescue–Kershenbaum–Ydstie (FKY) RLS forgetting factor (Fortescue et al., 1981) into the EKF error covariance measurement update:

$$P_k(+) = \frac{1}{\lambda_k}[I - K_k H_k(-)]P_k(-) \tag{8}$$

$$K_k = \frac{P_k(-)H_k^T(-)}{R_k + H_k(-)P_k(-)H_k^T(-)} \tag{9}$$

$$\tilde{\lambda}_k = 1 - \frac{1}{\sigma}\frac{[z_k - h_k(\hat{\underline{x}}_{k-1})]^2}{1 + H_k P_k H_k^T} \tag{10}$$

$$\lambda_k = \max\{\tilde{\lambda}_k, \lambda_{\min}\}, \qquad 0 < \lambda_{\min} \le 1, \tag{11}$$

where $\underline{x}$ is the state vector, K the update gain matrix, P the error covariance, R the measurement noise variance, z the measured output, $h(\hat{\underline{x}})$ the estimated output based on the estimated parameter values, H the Jacobian of the output with respect to the parameters, $\lambda_{\min}$ the user-defined minimum forgetting value, σ a forgetting factor tuning parameter, subscript k refers to the kth sampling instant, $(-)$ indicates the state variables or the covariance matrix after the time update, and $(+)$ indicates the state and covariance after the measurement update. The measurement update of the states and the time update equations are those of the standard continuous-discrete EKF (Gelb, 1974).

Since $\lambda_{\min} \le \lambda_k \le 1$, incorporation of the forgetting factor multiplies the error covariance matrix by a scalar value greater than one, thus increasing the gain. This increases the adjustment made to the state variable vector during the measurement update, that is, it makes the filter more sensitive to deviations between the actual and estimated outputs, allowing the filter to better deal with sudden changes in the state variables not predicted by the simple model.

Results

ZnTe/GaAs system

The EKF using only the simple model was applied to the ZnTe/GaAs system. This run was designed to have sudden changes in the film growth rate by changing the bubbler flow rate. Reflectance intensity drift and bias also showed sudden changes as well as considerable amounts of process and measurement noise. Process noise was largely due to the substrate rotation, done to promote epitaxial film thickness uniformity. However, because of unavoidable defects, the rotation produced noise with a frequency corresponding to the rotation rate ($\sim$ 3 cycles/min). The EKF was tuned with the parameters shown in Table 1. The measurement noise variance R was calculated from the variance of steady-state measurements before the growth run. The states were initialized at zero thickness, bias, and drift, and at a reasonable guess for growth rate. The diagonal elements of the initial error covariance $P(0)$ were set after an initial run with a high-valued diagonal $P(0)$ reached quasi-steady state. Off-diagonal

Table 1. Modified EKF Settings for the ZnTe/GaAs System

$\hat{\underline{x}}(0)$	$\begin{bmatrix} \theta(0) \\ g(0) \\ \alpha(0) \\ \beta(0) \end{bmatrix} = \begin{bmatrix} 0 \\ 0.2 \\ 0 \\ 0 \end{bmatrix}$
σ	2
Q	$\begin{bmatrix} 0.001 & 0 & 0 & 0 \\ 0 & 10^{-10} & 0 & 0 \\ 0 & 0 & 10^{-10} & 0 \\ 0 & 0 & 0 & 10^{-30} \end{bmatrix}$
R	0.000912
$P(0)$	$\begin{bmatrix} 0.1 & 0.001 & 0 & 0 \\ 0.001 & 0.001 & 0 & 0 \\ 0 & 0 & 10^{-30} & 0 \\ 0 & 0 & 0 & 10^{-18} \end{bmatrix}$
λ_{min}	0.9

elements were set to zero except for the ones relating thickness and growth rate, which have high interaction. Q was chosen diagonal with very small magnitudes except for the component corresponding to thickness, which was expected to have significant variance. A minimum forgetting-factor value of 0.9 is known to be successful in many applications and the other forgetting-factor parameter, σ, was set by trial and error.

A plot of measured and estimated reflectance vs. time (Figure 2) shows that the estimated reflectance follows the experimental curve extremely well, even though there are sudden jumps in the drift and bias, for example, at elasped time $\approx$ 3,200 s. An expanded view (Figure 3) illustrates the ability of the EKF to filter out much of the rotational noise.

During the run it was possible to find average growth rates over a period of time. Reflectance intensity from a growing film oscillates with a cycle corresponding to a constant change in thickness $\Delta\theta$, which is determined by the refractive index of the film n_f with

$$\Delta\theta = \frac{\lambda^*}{2n_f}, \tag{12}$$

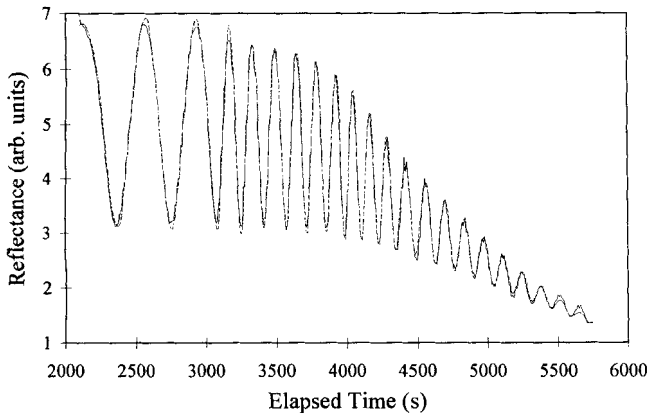

Figure 2. Measured reflectance (——) and EKF-estimated reflectance using the simple model (---) for the ZnTe/GaAs system.

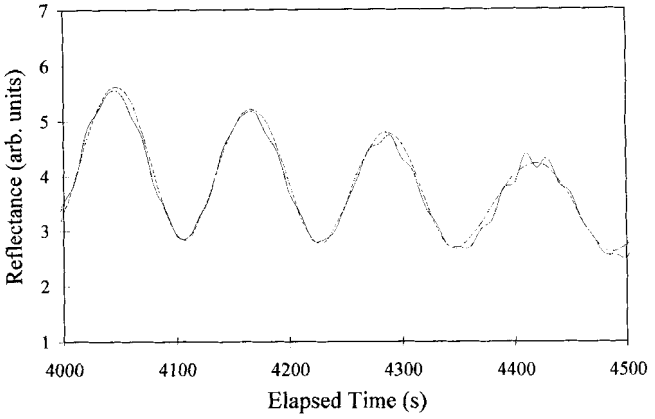

Figure 3. Expanded view of the measured reflectance (——) and EKF-estimated reflectance using the simple model (---) for the ZnTe/GaAs system.

where λ^* is the wavelength of the laser light (Irvine et al., 1992). For a zinc telluride film with a 6,328-Å laser, $\Delta\theta$ = 1,034 Å. Therefore, an average growth rate can be found by measuring the period or half-period of oscillations. To protect against extraneous extrema, the reflectance was filtered (here a fourth-order low pass was used) before calculating the average growth rate. The total film thickness can also be estimated by counting the total number of oscillations during the growth period. In the following discussion, extrema method refers to this method of estimating film thickness and growth rate.

Figure 4 is a plot of the estimated growth rate with the solid line being the EKF estimated growth rate, and the asterisks being the average growth rate determined by the extrema method. The agreement between the two methods is good. Late in the run, however, the latter method breaks down because the amplitude of the rotational noise becomes comparable to that of the oscillations due to growth, thus producing false extrema.

An item that should be noted is the steplike nature of the EKF-estimated growth rate. Instead of a smooth first-order

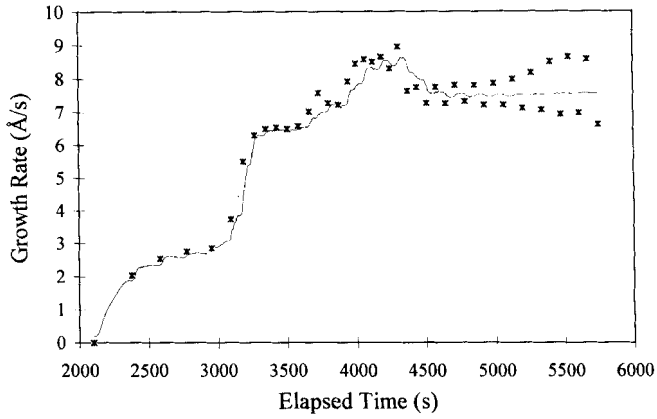

Figure 4. EKF-estimated growth rate (——) using the simple model for the ZnTe/GaAs system (the asterisks are the average growth rate between low-pass filtered reflectance extrema).

Table 2. Modified EKF Settings for the AlAs/GaAs System

	Simple Model	Improved Model
$\hat{x}(0)$	$\begin{bmatrix}\theta(0)\\ g(0)\\ \alpha(0)\\ \beta(0)\end{bmatrix}=\begin{bmatrix}0\\0\\0\\0\end{bmatrix}$	$\begin{bmatrix}\theta(0)\\ C_{Al}(0)\\ \alpha(0)\\ \beta(0)\\ \gamma(0)\end{bmatrix}=\begin{bmatrix}0\\0\\0\\0\\2.1\times10^{5}\end{bmatrix}$
σ	0.05	5
Q	$\begin{bmatrix}0.001&0&0&0\\0&0.001&0&0\\0&0&0&0\\0&0&0&0\end{bmatrix}$	$\begin{bmatrix}0.01&0&0&0&0\\0&10^{-14}&0&0&0\\0&0&0&0&0\\0&0&0&0&0\\0&0&0&0&0.1\end{bmatrix}$
R	0.001	0.001
$P(0)$	$\begin{bmatrix}0.1&0&0&0\\0&0.01&0&0\\0&0&10^{-10}&0\\0&0&0&10^{-7}\end{bmatrix}$	$\begin{bmatrix}0.01&0&0&0&0\\0&10^{-10}&0&0&0\\0&0&10^{-10}&0&0\\0&0&0&10^{-7}&0\\0&0&0&0&0.01\end{bmatrix}$
λ_{min}	0.9	0.9

response that might be expected, the response is made up of a series of small steps that approximate the smooth response. This is due to the loss of observability at the reflectance extrema, that is, the EKF can no longer sense differences between the actual and estimated states because a small change in the states results in no noticeable difference in the output. This effect can also be seen in Figure 3. The greatest deviation between the estimated and measured reflectance is found close to the extrema where the EKF cannot realign the curves. When observability is lost, the EKF must rely totally on the process model until observability is regained. Since the frequency of the reflectance intensity is a function of wavelength, the problem of loss of observability can be overcome using different colored lasers or spectral reflectometry (Killeen and Breiland, 1994). Then, observability would always be maintained at some wavelength.

The thickness calculated by counting the oscillations and the EKF-estimated thickness also closely agree. The final film thickness is 22,231 Å, corresponding to twenty-one and one-half oscillations, according to the extrema method, and 22,332 Å using the modified EKF.

AlAs/GaAs system

The modified EKF was also tested with two growth runs of the AlAs/GaAs system. The reflectance intensity for these data shows almost no noise, almost constant drift, and negligible bias. The time and magnitude of the bubbler flow rate changes were known and coincided with local reflectance maxima. In run 1, the TMA bubbler flow rate was initially stepped up to 12 std. cm^3/min, and on the next three successive peaks, it was stepped up to 24, 36 and 48 std. cm^3/min, respectively. The bubbler flow was turned off at the final peak. In run 2, the bubbler flow rate was initially stepped up to 36 std. cm^3/min, and then was stepped down to 24, 12, and 0 std. cm^3/min at the next three successive peaks. Both runs had a 7.5-std. L/min blanket flow of H_2 and a 2.5 std. L/min TMA push flow of H_2. In the following discussion, EKF-simple refers to the EKF using the simple model and EKF-improved to the EKF utilizing the improved model.

Table 2 shows the values of the EKF tuning parameters. They were obtained following a procedure along the lines previously discussed. In run 1, the experimental (solid line in Figure 5) and estimated reflectance (dashed line in Figure 5) showed good agreement with the greatest deviation occurring at the beginning of the growth run, at the next successive peak, and at the end, where there were the largest relative growth rate changes. These deviations were due to the fact that the model does not predict any changes in growth rate making the filter completely reactive. The plot of estimated growth rate (Figure 6) clearly reflects the step changes made in the TMA bubbler flow rate. The asterisks are the average growth rate using the extrema method where one full oscillation corresponds to 1,029 Å. The asterisks appear at the end of the time interval from which they were calculated. There-

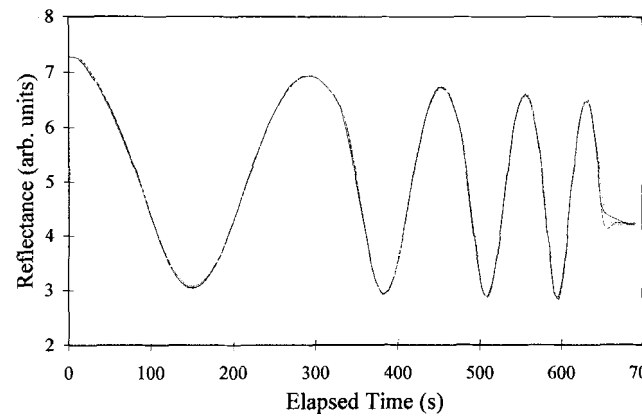

Figure 5. Measured and estimated reflectance for run 1 of the AlAs/GaAs system (——, measured; – – –, EKF-simple; · · · ·, EKF-improved).

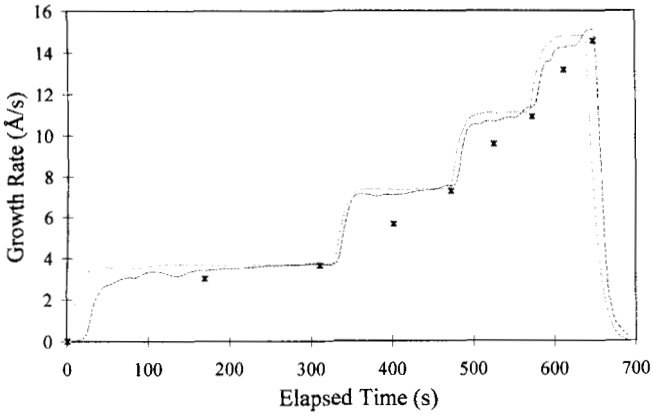

Figure 6. Estimated growth rate for run 1 of the AlAs/GaAs system (---, EKF-simple; ····, EKF-improved; *, average growth rate between filtered reflectance extrema).

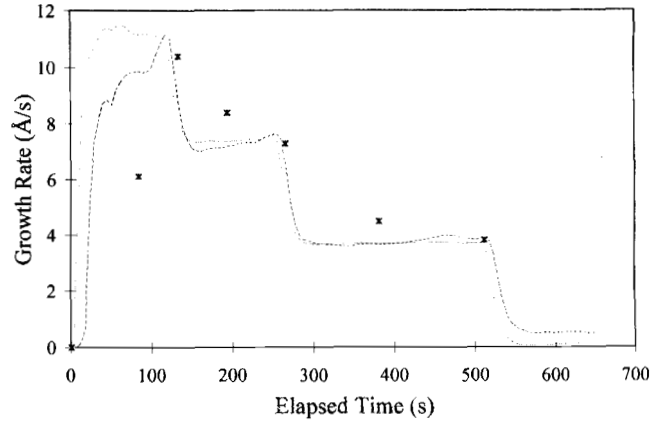

Figure 8. Estimated growth rate for run 2 of the AlAs/GaAs system (---, EKF-simple; ····, EKF-improved; *, average growth rate between filtered reflectance extrema).

fore, in intervals in which there was a large change in growth rate, there was a large difference between the average and final growth rate. Taking the placement of the asterisks into account, and the delays associated with low-pass filtering, the agreement between the EKF-simple estimated growth rate and the extrema-method growth rate estimate is good. A thickness of 4,425 Å using the extrema method (corresponding to 4.3 oscillations) closely agrees with the 4,365 Å estimated by the EKF-simple.

Figures 7 and 8 show the performance of the EKF-simple for run 2, when tuned with the same parameters as run 1 (Table 2). The reflectance (Figure 7) again shows good agreement, with some deviation during the first and fourth maxima. The growth rate estimate (dashed line in Figure 8) is less successful than in run 1 at tracking the initial step change (which is three times the magnitude of the corresponding change in run 1). Nevertheless, the EKF does track the step changes in growth rate and also produces a thickness estimate of 3,231 Å, which is close to that of the extrema method estimate of 3,190 Å.

The EKF-improved was tuned with the parameters shown in Table 2. The reflectance for run 1 (dotted line in Figure 5) shows very good agreement with experimental measurement, as was the case for EKF-simple. The growth rate (dotted line in Figure 6) clearly shows the step changes and is close to that for EKF-simple; it does, however, conform closer to what would be theoretically expected, and since the improved model predicts changes in growth rate, the filter does not suffer as badly from the temporary loss of observability. The final estimated thickness of 4,372 Å is essentially equal to that of EKF-simple.

The dotted lines in Figures 7 and 8 show the reflectance and growth rates for run 2 using EKF-improved when tuned with the same parameters as in run 1 (Table 2). The reflectance agrees well with the experimental data and is comparable to the profile obtained with EKF-simple. The growth rate clearly shows the step changes and does not run into difficulty at the points of loss of observability. The final thickness estimate of 3,224 Å is essentially equal to that of the EKF-simple.

Conclusion

The successful performance of EKF-improved is expected, as the filter relies on a model that predicts the process

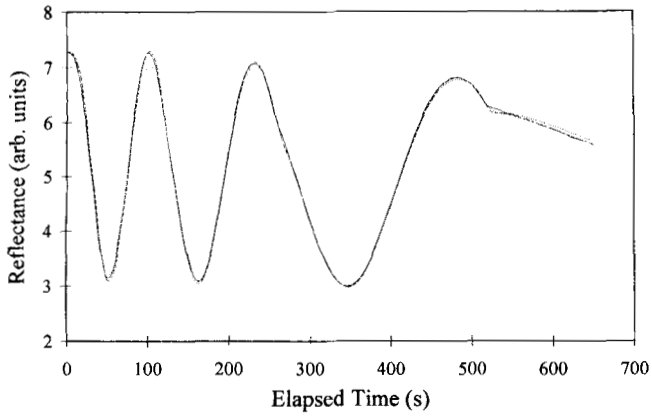

Figure 7. Measured and estimated reflectance for run 2 of the AlAs/GaAs system (——, measured; ---, EKF-simple; ····, EKF-improved).

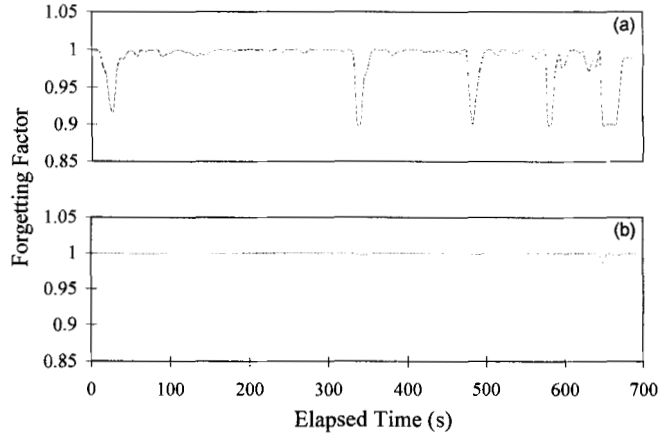

Figure 9. Forgetting factor for run 1 of the AlAs/GaAs system for (a) EKF-simple and (b) EKF-improved.

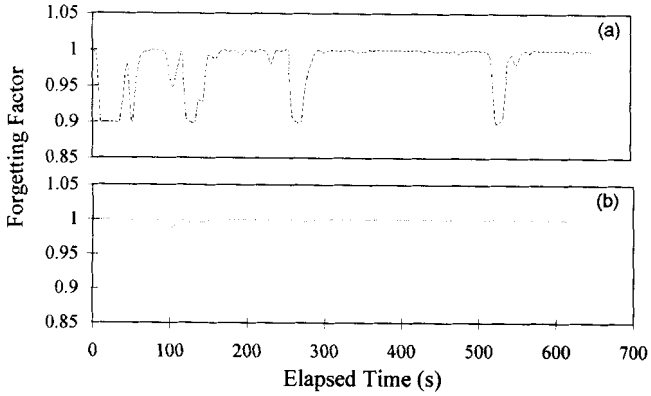

Figure 10. Forgetting factor for run 2 of the AlAs/GaAs system for (a) EKF-simple and (b) EKF-improved.

changes. The EKF-simple is almost as successful, even though the model assumes a constant growth rate. The reason for this can be seen by looking at the behavior of the forgetting factor λ_k. In run 1, the EKF-simple depends heavily on the forgetting factor to correct the state variables so as to better agree with the output (Figure 9a). When the growth rate changes, the forgetting factor often reaches the lower limit λ_{min} of 0.9. The EKF-improved does not depend on the forgetting factor. The model's ability to predict changes in growth rate gives the filter more than one mechanism to track the states, thus keeping the forgetting factor close to one (Figure 9b), practically eliminating forgetting. Similar results were obtained when run 2 data were used (Figure 10), except that for both models more forgetting was observed. Incorporation of the forgetting factor, then, allows the EKF to overcome some of the shortcomings of the available process model. It should also be remarked that the better the model is, the easier it is to tune the EKF for satisfactory performance.

Acknowledgment

The authors at the University of Florida gratefully acknowledge support from Rockwell International Corporation.

Literature Cited

Alius, H., and R. Schmidt, "Interference Method for Monitoring the Refractive Index and the Thickness of Transparent Films During Deposition," *Rev. Sci. Instrum.*, **61**, 1200 (1990).

Åström, K. J., and B. Wittenmark, *Adaptive Control*, Addison-Wesley, Reading, MA (1988).

Bajaj, J., S. J. C. Irvine, H. O. Sankur, and S. A. Svoronos, "Modeling of In Situ Monitored Laser Reflectance During MOCVD Growth of HgCdTe," *J. Electron. Mat.*, **22**, 899 (1993).

Boebel, F. G., and H. Möller, "Simultaneous In Situ Measurement of Film Thickness and Temperature by Using Multiple Wavelengths Pyrometric Interferometry (MWPI)," *IEEE Trans. Semicond. Manuf.*, **SM-6**, 112 (1993).

Boning, D. S., J. L. Claman, K. S. Wong, T. J. Dalton, and H. H. Sawin, "Plasma Etch Endpoint via Interferometric Imaging," *Proc. Amer. Contr. Conf.*, p. 897 (1994).

Breiland, W. G., T. M. Brennan, H. C. Chui, B. E. Hammons, and K. P. Kileen, "Normal Incidence Reflectance: A Robust Tool for *In-Situ* Real-Time Measurement of Growth Rates and Optical Constants of CVD-Grown Semiconductor Thin Films," Paper No. 98, Electrochem. Soc. Meet., Reno, NV (1995).

Deaton, R., and A. George, "Quantification of Laser Interference Fringes as Applied to Plasma Etch Endpoint Detection," *SPIE Proc. Lasers in Microlithography*, **774**, 162 (1987).

Fortescue, T. R., L. S. Kershenbaum, and B. E. Ydstie, "Implementation of Self-Tuning Regulators with Variable Forgetting Factors," *Automatica*, **17**, 831 (1981).

Gelb, A., *Applied Optimal Estimation*, MIT Press, Cambridge, MA (1974).

Goodwin, G. C., and K. S. Sin, *Adaptive Filtering Prediction and Control*, Prentice-Hall, Englewood Cliffs, NJ (1984).

Irvine, S. J. C., J. Bajaj, and R. V. Gil, "Integrated In Situ Monitoring of a Metalorganic Vapor Phase Reactor for II-VI Epitaxy," *J. Electron. Mat.*, **23**, 167 (1994).

Irvine, S. J. C., J. Bajaj, and H. O. Sankur, "Complete In-Situ Monitoring of MOCVD HgCdTe/CdTe/ZnTe Growth on GaAs Substrates," *J. Crystal Growth*, **21**, 654 (1992).

Irvine, S. J. C., H. Hill, G. T. Brown, S. J. Barnett, J. E. Hails, O. D. Dosser, and J. B. Mullin, "Selected Area Epitaxy in II-VI Compounds by Laser-Induced Photometalorganic Vapor Phase Epitaxy," *J. Vac. Sci. Technol. B*, **7**, 1191 (1989).

Jensen, J. E., P. D. Brewer, G. L. Olson, L. W. Tutt, and J. J. Zinck, "Excimer Laser-Assisted Metalorganic Vapor Phase Epitaxy of CdTe and HgTe on (100) GaAs," *J. Vac. Sci. Technol. A*, **6**, 2808 (1988).

Killeen, K. P., and W. G. Breiland, "In Situ Spectral Reflectance Monitoring of III-V Epitaxy," *J. Electron. Mat.*, **23**, 179 (1994).

Macleod, H. A., *Thin Film Optical Filters*, 2nd ed., Macmillan, New York (1986).

Morrison, P. W., "A Method to Determine the Infrared Optical Constants and Thickness of a Thin Film from a Single Reflectance Spectrum," Paper no. 97, Electrochem. Soc. Meet., Reno, NV (1995).

Rhiger, D. R., "Use of Ellipsometry to Characterize the Surface of HgCdTe," *J. Electron. Mat.*, **22**, 887 (1993).

Sankur, H., W. Southwell, and R. Hall, "In Situ Optical Monitoring of OMVPE Deposition of AlGaAs by Laser Reflectance," *J. Electron. Mat.*, **20**, 1099 (1991).

Sternheim, M., W. van Gelder, and A. W. Hartman, "A Laser Interferometer System to Monitor Dry Etching of Patterned Silicon," *J. Electrochem. Soc.*, **130**, 655 (1983).

Wang, X. G., G. A. Dumont, and M. S. Davies, "Estimation in Paper Machine Control," *IEEE Contr. Sys.*, **CS-13**, 34 (1993).

Wong, K. S., and D. S. Boning, "On In Situ Etch Rate Extraction from Interferometric Signals," Paper no. 114, Electrochem. Soc. Meet., Reno, NV (1995).

Manuscript received Mar. 16, 1995, and revision received Aug. 16, 1995.